Lattice Effects in the Mössbauer Spectra of Salts of $[Fe_4S_4(SBu^t)_4]^{2-}$. Crystal Structures of $[NMe_4]_2[Fe_4S_4(SBu^t)_4]\cdot HSBu^t$ and $[N(n\text{-}C_5H_{11})_4]_2[Fe_4S_4(SBu^t)_4]\cdot HSBu^t$*

David J. Evans, Adrian Hills, David L. Hughes, and Geoffrey J. Leigh
AFRC IPSR Nitrogen Fixation Laboratory, University of Sussex, Brighton BN1 9RQ
Andrew Houlton and Jack Silver
Department of Chemistry and Biological Chemistry, University of Essex, Wivenhoe Park, Colchester CO4 3SQ

The Mössbauer spectra of salts containing the anions $[Fe_4S_4(SBu^t)_4]^{2-}$ or $[FeX_4]^{2-}$ (X = Cl or Br) show relatively invariant isomer shifts, but quadrupole splittings which are cation-dependent, for example varying from 0.84 to 1.32 mm s^{-1} for $[NR_4]_2[Fe_4S_4(SBu^t)_4]$. This observation is rationalized in terms of perturbations exerted by the cations on the field gradient at the iron centres. As aids to this rationalization, the *X*-ray crystal structures of $[NMe_4]_2[Fe_4S_4(SBu^t)_4]\cdot HSBu^t$ and of $[N(n\text{-}C_5H_{11})_4]_2[Fe_4S_4(SBu^t)_4]\cdot HSBu^t$ were determined.

An understanding of the properties of the metal clusters in ferredoxins and high-potential iron proteins has been a primary concern in the development of the chemistry of iron-sulphur clusters. We have been particularly interested in $Fe_4S_4^{2+}$ clusters such as are found in *Pseudomonas aerogenes* ferredoxin and in nitrogenases. The ^{57}Fe Mössbauer spectra of such clusters, both in natural systems and in models, exhibit a simple quadrupole doublet though the clusters formally contain two iron(II) and two iron(III) atoms.[1] This doublet has a relatively invariant isomer shift (i.s.) (*ca.* 0.40–0.50 mm s^{-1}), changing slightly with the ligands L in $[Fe_4S_4L_4]^{2-}$ (Table 1). However, the quadrupole splitting (q.s.) varies from salt to salt in a way not easy to rationalize. This variation has also been observed in biological systems (Table 2) where the ligands L are all cysteinato-residues of the protein. It has been ascribed to some kind of protein-cluster interaction.[2,3]

We have previously noted[4] that there is a dependence of the q.s. on the cation in salts of $[Fe_4S_4L_4]^{2-}$ (L = SBu^t). In order to understand this and to shed light on the mechanism of protein–cluster interactions, we have extended these observations to further cluster salts and to tetrahalogenoferrates(II). This paper discusses the new data.

Table 1. Mössbauer spectral data for some $Fe_4S_4^{2+}$ clusters (77 K)

Compound	Isomer shift/ mm s^{-1}	Quadrupole splitting/ mm s^{-1}
$[PPh_4]_2[Fe_4S_4(SPh)_4]$	0.43	0.93[a]
$[PPh_4]_2[Fe_4S_4(SBu^t)_4]$	0.44(1)	0.97(1)[b]
$[PPh_4]_2[Fe_4S_4Cl_4]$	0.49	0.67[a]
$[NMe_4]_2[Fe_4S_4Cl_4]$	0.50(1)	0.98(1)[b]
$[NEt_4]_2[Fe_4S_4Cl_4]$	0.50(1)	1.06(1)[b]

[a] M. G. Kanatzidis, N. C. Baenziger, D. Coucouvanis, A. Simopoulos, and A. Kostikas, *J. Am. Chem. Soc.*, 1984, **106**, 4500. [b] This work

Table 2. Mössbauer spectral data for some $Fe_4S_4^{2+}$ ferredoxins (77 K)[3]

Source	Isomer shift/ mm s^{-1}	Quadrupole splitting/ mm s^{-1}
Bacillus stearothermophilus	0.42(1)	0.98(2)
Clostridium pasteurianum	0.43(1)	0.91(1)
Chromatium (high-potential iron protein)	0.42(1)	1.13(1)

Results and Discussion

We have been interested in the binding of amino acids other than cysteine to $Fe_4S_4^{2+}$ clusters, and incidentally prepared a number of salts of the anion $[Fe_4S_4(SBu^t)_4]^{2-}$.[5] The Mössbauer data are presented in Table 3, which includes data for a caesium salt and for a single $[Fe_4Se_4(SBu^t)_4]^{2-}$ derivative. From the table the following points are apparent. (*i*) The i.s. are similar though not constant, so that there may be a small cation dependence. (*ii*) There is a large variation in the quadrupole splittings, far larger than three standard deviations of the experimental errors. For example, the tetra-alkylammonium salts have quadrupole splittings which vary between 0.84(1) and 1.32(1) mm s^{-1}, with a maximum at the $[NPr^n_4]^+$ salt.

In simple discussions the i.s. is taken to represent a measure of the electron density at the nucleus.[6] This electron density could be affected by bonding directly involving the *s* electrons, or by changes in the shielding due to *p* and *d* electrons. Only a small influence on i.s. is observed, presumably operating in these ionic compounds by the latter mechanism.

The q.s. arises from the electric field gradient (V_{zz}) around the iron nuclei. This is taken to be the sum of the valence term q_{val}, which arises from asymmetric electron distribution about the nuclei, and the lattice term q_{latt} arising from the distribution of other charges in the neighbourhood of the nuclei. Usually, these are taken to be of opposite sign, and $|q_{val}| \gg |q_{latt}|$.

The data of Table 3 suggest that in our salts this is not the case and the q.s. must be influenced by q_{latt} to a considerable degree. This should be a general effect not clearly recognized hitherto. To check whether the effect might be recognizable from the solid, we decided to determine specimen structures. The crystal structure of $[NEt_4]_2[Fe_4S_4(SBu^t)_4]$ has already been reported.[7] Here we report the structures of the $[NMe_4]^+$ and $[N(n\text{-}C_5H_{11})_4]^+$ salts.

Description of the Structures of $[NR_4]_2[Fe_4S_4(SBu^t)_4]$ (R = Me or n-C_5H_{11}).—The tetramethylammonium salt has the same space-group symmetry ($I\bar{4}2m$, no. 121) as, and very similar cell dimensions to, the tetraethylammonium salt reported by Holm and co-workers,[7] and these two may be

* *Supplementary data available:* see Instructions for Authors, *J. Chem. Soc., Dalton Trans.*, 1990, Issue 1, pp. xix—xxii.

Table 3. Mössbauer spectral data for salts containing $[Fe_4S_4(SBu^t)_4]^{2-}$ (77 K)

Cation	Isomer shift/ mm s^{-1}	Quadrupole splitting/ mm s^{-1}	Linewidth/ mm s^{-1}
$[NMe_4]^+$	0.46(1)	0.84(1)	0.30(1)
$[NEt_4]^+$	0.43(1)	1.14(1)	0.23(1)
$[NPr^n_4]^+$	0.43(1)	1.32(1)	0.14(1)
$[NBu^n_4]^+$	0.44(1)	1.22(1)	0.21(1)
$[N(n\text{-}C_5H_{11})_4]^+$	0.43(1)	1.29(1)	0.30(1)
$[N(n\text{-}C_6H_{13})_4]^+$	0.43(1)	1.25(1)	0.20(1)
$[PMe_4]^+$	0.39(1)	0.93(1)	0.17(1)
$[PEt_4]^+$	0.39(1)	0.92(1)	0.19(1)
$[PPr^n_4]^+$	0.40(1)	1.13(1)	0.19(1)
$[PBu^n_4]^+$	0.39(1)	1.25(1)	0.17(1)
$[NMe_3(CH_2Ph)]^+$	0.43(1)	1.10(1)	0.19(1)
$[NEt_3(CH_2Ph)]^+$	0.43(1)	1.16(1)	0.16(1)
$[NPr^n_3(CH_2Ph)]^+$	0.42(1)	1.34(1)	0.14(1)
$[NBu^n_3(CH_2Ph)]^+$	0.43(1)	1.10(1)	0.24(1)
Cs^+	0.42(1)	0.84(1)	0.27(1)
$[NBu^n_4]_2[Fe_4Se_4(SBu^t)_4]$	0.46(1)	1.37(1)	0.14(1)

Table 4. Molecular dimensions for $[NMe_4]_2[Fe_4S_4(SBu^t)_4]\cdot HSBu^t$ (distances in Å, angles in °) with estimated standard deviations (e.s.d.s) in parentheses

(*a*) In the anion

Fe–Fe^I	2.741(2)	S(2)–C(1)	1.847(14)
Fe–Fe^{II}	2.741(2)	C(1)–C(2a)	1.628(25)
Fe–S(1)	2.321(3)	C(1)–C(3a)	1.46(5)
Fe–$S(1^{II})$	2.278(3)	C(1)–C(2b)	1.50
Fe–S(2)	2.261(3)	C(1)–C(3b)	1.50
Fe^I–Fe–Fe^{II}	60.0(1)	Fe–S(1)–Fe^{II}	73.2(1)
Fe^I–Fe–S(1)	100.3(1)	Fe^{II}–S(1)–Fe^{III}	74.0(1)
Fe^I–Fe–$S(1^{II})$	53.0(1)	Fe–S(2)–C(1)	112.7(4)
Fe^I–Fe–S(2)	158.8(1)	S(2)–C(1)–C(2a)	107.3(11)
Fe^{II}–Fe–Fe^{III}	60.0(1)	S(2)–C(1)–C(3a)	104.8(12)
Fe^{II}–Fe–S(1)	52.7(1)	S(2)–C(1)–C(2b)	110.1
Fe^{II}–Fe–$S(1^{II})$	54.1(1)	S(2)–C(1)–C(3b)	110.1
Fe^{II}–Fe–$S(1^{III})$	101.4(1)	C(2a)–C(1)–C(3a)	103.1(17)
Fe^{II}–Fe–S(2)	136.2(1)	C(3a)–C(1)–$C(3a^{IV})$	131.9(23)
S(1)–Fe–$S(1^{II})$	104.9(1)	C(2b)–C(1)–C(3b)	109.5
S(1)–Fe–S(2)	100.9(1)	C(3b)–C(1)–$C(3b^{IV})$	107.7
$S(1^{II})$–Fe–$S(1^{III})$	103.3(1)		
$S(1^{II})$–Fe–S(2)	120.4(1)		

(*b*) In the cation

N(4)–C(4)	1.501(16)	C(4)–N(4)–$C(4^V)$	107.9(8)
		C(4)–N(4)–$C(4^{VI})$	109.7(9)
		C(4)–N(4)–$C(4^{VII})$	110.8(9)

(*c*) In the disordered $HSBu^t$ molecule

C(5)–C(51)	1.52(3)	C(51)–C(5)–$C(51^I)$	99.2(18)
C(5)–S(51)	1.855(22)	C(51)–C(5)–$C(51^{VII})$	114.8(15)
		C(51)–C(5)–$S(51^I)$	113.8(16)
		C(51)–C(5)–$S(51^{VII})$	106.4(13)

The Roman superscripts denote symmetry-related positions: I $1-x, 1-y, z$; II $1-x, y, 1-z$; III $x, 1-y, 1-z$; IV y, x, z; V $-x, 1-y, z$; VI $-x, y, -z$; VII $x, 1-y, -z$.

considered isostructural as far as the ionic components are concerned. Both compounds are apparently also isostructural with the tetrapropylammonium cluster, which we did not investigate further. In each crystal, the ammonium cations lie on points of 222 symmetry and the $[Fe_4S_4(SBu^t)_4]^{2-}$ anion (Figure 1) has its centre at an adjacent $\bar{4}2m$ symmetry point. The

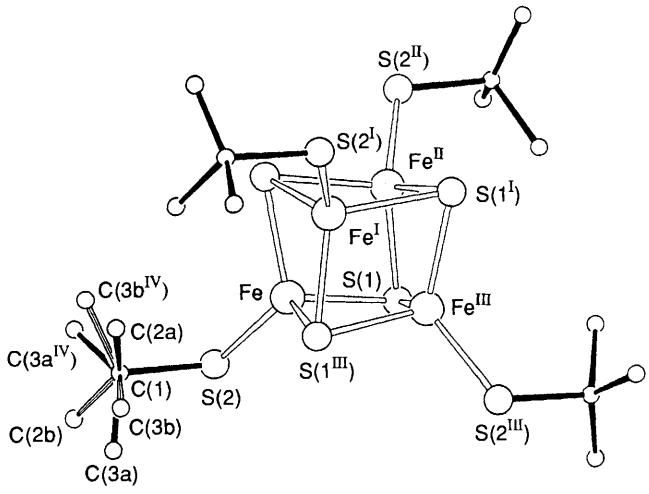

Figure 1. The anion in $[NMe_4]_2[Fe_4S_4(SBu^t)_4]\cdot HSBu^t$, showing the atom-labelling scheme. A precise $\bar{4}$-symmetry axis lies nearly horizontal in the plane of the projection. Each of the t-butyl groups is disordered in two orientations, but, for clarity, both arrangements are shown only for one group

dimensions in the two anions are very similar, and those for the $[NMe_4]^+$ salt are listed in Table 4. There are, however, free molecules of the thiol $HSBu^t$ in the lattice of the $[NMe_4]^+$ salt; in the crystals of the $[NEt_4]^+$ salt four ethyl groups from separate cations converge towards the site corresponding to that occupied by the thiol in the $[NMe_4]^+$ salt and there is no room there for a thiol molecule. Atomic co-ordinates for the $[NMe_4]^+$ salt are in Table 5.

In the tetrapentylammonium crystals there is no symmetry within the $[Fe_4S_4(SBu^t)_4]^{2-}$ anion (Figure 2) and there are two independent cations; there are also disordered, unresolved molecules in the lattice thought to be $HSBu^t$. Molecular dimensions are listed in Table 6 and atomic co-ordinates in Table 7. The anion has the well established cubane-type Fe_4S_4 core, with dimensions very similar to those in the tetramethylammonium salt and others tabulated by Holm and co-workers.[7] As detailed previously,[4] the cluster shows good pseudo $\bar{4}$ symmetry, with distortions parallel to the pseudo-$\bar{4}$ axis. Each iron atom subtends a single bond from the Fe_4S_4 cluster to a thiolate ligand; this bond is not far removed from the pseudo-three-fold axis through the cluster; the slight distortion from linearity is very similar in each of the four bonds and the mean $S_{nn}\cdots Fe_n\text{–}S_n$ angle (see Figure 2) is 176.7(4)°, the deviation being much less here than in the $[NMe_4]^+$ and $[NEt_4]^+$ salts [165.3(1) and 173.2(1)°, respectively]. This is presumably related to different arrangements of the SBu^t groups. In the crystals of the $[NMe_4]^+$ and $[NEt_4]^+$ salts the symmetry requires the SBu^t groups to lie in the mirror plane (which passes through the cluster), whereas in the $[N(n\text{-}C_5H_{11})_4]^+$ salt there is no such restriction and the SBu^t groups are displaced from the plane; the C–S–Fe ··· Fe′ torsion angle [*e.g.* C(1)–S(1)–Fe(1) ··· Fe(4)] has a mean absolute value of 16(2)°.

In the crystals of the tetramethyl- and tetrapentyl-ammonium salts, and probably in the tetraethylammonium salt too, there is rotational disorder in the butyl groups showing (at least) two sites for each methyl group, formed by rotation about the apparently fixed S–C bond. The general orientation of the thiolate ligands is very similar in all three crystals, *viz.* the S–C bonds are all roughly parallel to the $\bar{4}$ symmetry axis (exact or pseudo); this contrasts with the $[NMe_3(CH_2Ph)]^+$ salt, where three bonds are close to being parallel and one is normal to these.[7]

Table 5. Final atomic co-ordinates (fractional × 10^4) for $[NMe_4]_2[Fe_4S_4(SBu^t)_4]\cdot HSBu^t$ with e.s.d.s in parentheses

Atom	*x*	*y*	*z*	S.o.f.*
Fe	4 156(1)	4 156(1)	4 467.2(8)	
S(1)	3 900(2)	3 900(2)	5 722(2)	
S(2)	2 858(2)	2 858(2)	4 018(2)	
C(1)	2 829(11)	2 829(11)	3 003(7)	
C(2a)	3 778(19)	3 778(19)	2 714(13)	0.75
C(3a)	1 713(21)	3 360(50)	2 803(12)	0.75
C(2b)	1 953(13)	1 953(13)	2 740(8)	0.25
C(3b)	2 519(22)	4 010(14)	2 710(6)	0.25
N(4)	0	5 000	0	
C(4)	742(15)	4 247(14)	485(8)	
C(5)	5 000	5 000	0	
C(51)	4 288(22)	4 288(22)	541(21)	0.75
S(51)	3 971(15)	3 971(15)	444(19)	0.25

* Site occupancy factor, if less than 1.0

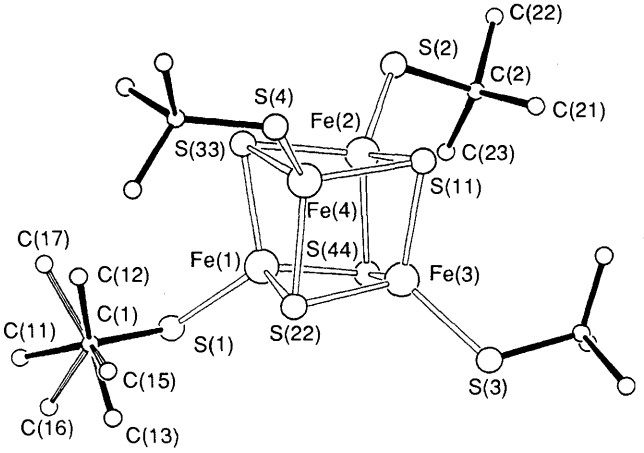

Figure 2. The anion in $[N(n\text{-}C_5H_{11})_4]_2[Fe_4S_4(SBu^t)_4]\cdot n HSBu^t$, showing the atomic labelling scheme. The orientation is similar to that in Figure 1, with the pseudo-$\bar{4}$-symmetry axis nearly horizontal in the diagram. Again, each of the t-butyl groups is disordered, and both orientations are shown only for the S(1) group

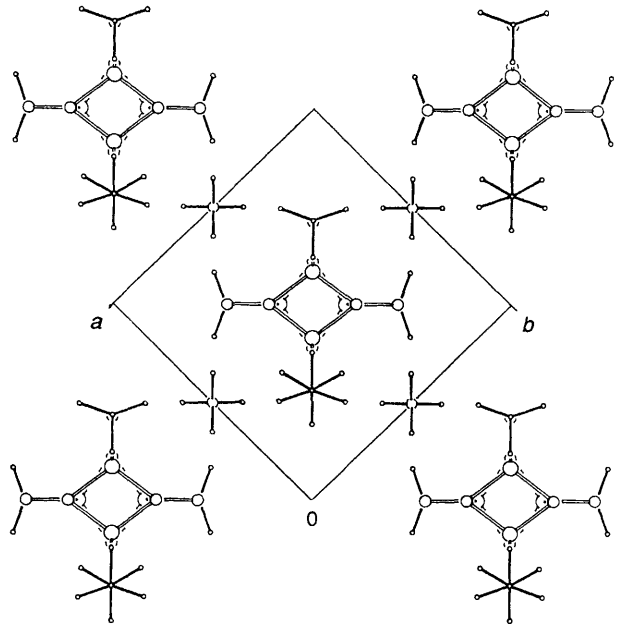

Figure 3. View down the $\bar{4}$-symmetry axis of $[NMe_4]_2[Fe_4S_4(SBu^t)_4]\cdot HSBu^t$. The two orientations are shown for only one of the t-butyl groups in each anion.

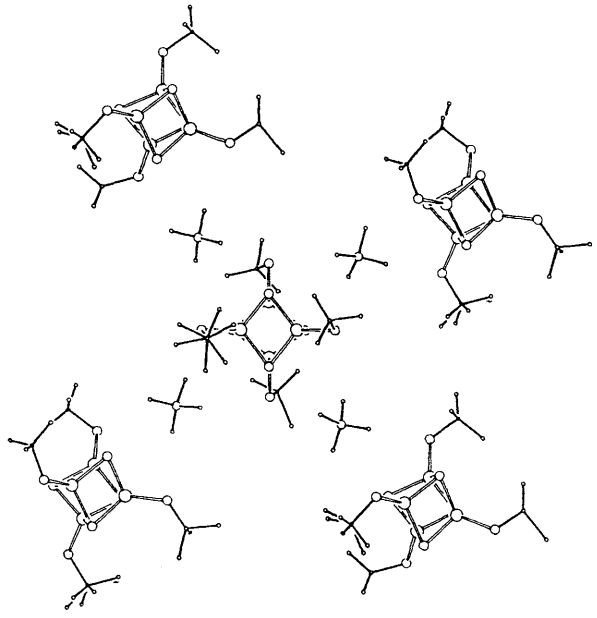

Figure 4. View down the pseudo-$\bar{4}$-symmetry axis of one anion (the central one) in $[N(n\text{-}C_5H_{11})_4]_2[Fe_4S_4(SBu^t)_4]\cdot n HSBu^t$. Both orientations for the disordered t-butyl groups in the anion are shown for only one group. For the cations, only the N and C_α atoms are shown. Note that the pseudo-$\bar{4}$-symmetry axes of the outer anions all lie approximately in the plane of projection

The interactions of the anions with neighbouring ions are very similar, too, in all three salts. In each case, there are four cations around the Fe_4S_4 core. In the symmetrical tetramethyl- and tetraethyl-ammonium crystals the four N atoms of the cations lie on the two-fold symmetry axes that pass through the centre of the Fe_4S_4 cluster and are normal to the $\bar{4}$ axis (Figure 3), whereas in the tetrapentylammonium salt the cations are displaced from this precise plane but are in generally similar positions (Figure 4). In all these crystals each core S atom has a cationic C_α atom at a distance rather less than that of a normal van der Waals contact (*ca.* 3.85 Å). The four S • • • C_α distances are in the range 3.47(2)—3.74(2) Å (pentyl) and at 3.66(2) (methyl) and 3.72(2) Å (ethyl).

We note also that each cation bridges linearly (exactly or approximately) two anions with the short S • • • C contacts and that there is thus a framework resulting from these strong anion–cation interactions. In the tetrapentylammonium salt (Figure 4) one anion is surrounded (in the plane approximately normal to the pseudo-$\bar{4}$ axis) by four cations which each contact another anion which is in the same plane; the $\bar{4}$ axes of this ring of connected anions are perpendicular to that of the central atom, and thus further short contacts from the anions to more cations extend the framework into three dimensions. This contrasts with the arrangements in the tetramethyl- and tetraethyl-ammonium salts (Figure 3), where all the $\bar{4}$ axes are crystallographically precise and parallel; in these crystals the extended anion–cation framework is thus two dimensional, forming layers, normal to the $\bar{4}$ axes, through the crystal.

In the two independent cations in the tetrapentylammonium salt all the C_5H_{11} chains are primarily elongated in all-*trans* conformations. However, there is considerable thermal motion in these chains, and several instances of site disorder were found, where there are alternative sites for the atoms of the chain. Complete resolution has not been possible in some chains, and the thermal parameters and molecular dimensions here are not satisfactory.

Table 6. Selected molecular dimensions for $[N(n\text{-}C_5H_{11})_4]_2[Fe_4S_4(SBu^t)_4]\cdot n HSBu^t$ (lengths in Å, angles in °) with e.s.d.s in parentheses

(*a*) In the anion

Fe(1)–Fe(2)	2.782(4)	Fe(2)–Fe(3)	2.793(4)	S(22)–Fe(1)–S(33)	103.2(2)	S(11)–Fe(3)–S(22)	103.2(2)
Fe(1)–Fe(3)	2.783(4)	Fe(2)–Fe(4)	2.781(4)	S(22)–Fe(1)–S(44)	103.1(2)	S(11)–Fe(3)–S(44)	105.2(2)
Fe(1)–Fe(4)	2.801(3)	Fe(3)–Fe(4)	2.765(4)	S(33)–Fe(1)–S(44)	104.8(2)	S(22)–Fe(3)–S(44)	102.6(2)
Fe(1)–S(22)	2.334(6)	Fe(3)–S(11)	2.288(6)	S(22)–Fe(1)–S(1)	116.0(2)	S(11)–Fe(3)–S(3)	116.4(3)
Fe(1)–S(33)	2.297(6)	Fe(3)–S(22)	2.291(7)	S(33)–Fe(1)–S(1)	117.0(2)	S(22)–Fe(3)–S(3)	109.9(3)
Fe(1)–S(44)	2.240(7)	Fe(3)–S(44)	2.297(6)	S(44)–Fe(1)–S(1)	111.2(2)	S(44)–Fe(3)–S(3)	117.8(3)
Fe(1)–S(1)	2.258(7)	Fe(3)–S(3)	2.272(7)	S(11)–Fe(2)–S(33)	101.9(2)	S(11)–Fe(4)–S(22)	103.6(2)
Fe(2)–S(11)	2.323(6)	Fe(4)–S(11)	2.237(7)	S(11)–Fe(2)–S(44)	103.2(2)	S(11)–Fe(4)–S(33)	104.6(2)
Fe(2)–S(33)	2.293(7)	Fe(4)–S(22)	2.328(6)	S(33)–Fe(2)–S(44)	102.2(2)	S(22)–Fe(4)–S(33)	103.6(2)
Fe(2)–S(44)	2.327(6)	Fe(4)–S(33)	2.292(6)	S(11)–Fe(2)–S(2)	117.7(2)	S(11)–Fe(4)–S(4)	110.7(2)
Fe(2)–S(2)	2.214(7)	Fe(4)–S(4)	2.254(7)	S(33)–Fe(2)–S(2)	111.5(2)	S(22)–Fe(4)–S(4)	116.2(2)
S(1)–C(1)	1.861(25)	S(3)–C(3)	1.827(30)	S(44)–Fe(2)–S(2)	118.1(2)	S(33)–Fe(4)–S(4)	116.7(2)
S(2)–C(2)	1.841(25)	S(4)–C(4)	1.840(30)	Fe(2)–S(11)–Fe(3)	74.6(2)	Fe(1)–S(33)–Fe(2)	74.6(2)
				Fe(2)–S(11)–Fe(4)	75.1(2)	Fe(1)–S(33)–Fe(4)	75.2(2)
				Fe(3)–S(11)–Fe(4)	75.3(2)	Fe(2)–S(33)–Fe(4)	74.7(2)
				Fe(1)–S(22)–Fe(3)	74.0(2)	Fe(1)–S(44)–Fe(2)	75.0(2)
				Fe(1)–S(22)–Fe(4)	73.9(2)	Fe(1)–S(44)–Fe(3)	75.7(2)
				Fe(3)–S(22)–Fe(4)	73.5(2)	Fe(2)–S(44)–Fe(3)	74.3(2)
				Fe(1)–S(1)–C(1)	113.1(9)	Fe(3)–S(3)–C(3)	112.8(10)
				Fe(2)–S(2)–C(2)	110.6(8)	Fe(4)–S(4)–C(4)	112.4(9)

(*b*) In the cations

N(5)–C(51)	1.539(29)	N(8)–C(81)	1.490(30)	C(51)–N(5)–C(56)	109.0(17)	C(81)–N(8)–C(86)	113.0(17)
N(5)–C(56)	1.65(3)	N(8)–C(86)	1.56(3)	C(51)–N(5)–C(61)	113.7(17)	C(81)–N(8)–C(91)	108.9(17)
N(5)–C(61)	1.53(3)	N(8)–C(91)	1.59(3)	C(56)–N(5)–C(61)	100.3(17)	C(86)–N(8)–C(91)	103.2(17)
N(5)–C(66)	1.53(3)	N(8)–C(96)	1.523(29)	C(51)–N(5)–C(66)	107.0(17)	C(81)–N(8)–C(96)	110.3(17)
C(51)–C(52)	1.51(3)	C(81)–C(82)	1.42(3)	C(56)–N(5)–C(66)	115.2(17)	C(86)–N(8)–C(96)	112.0(17)
C(56)–C(57)	1.51(4)	C(86)–C(87)	1.53(4)	C(61)–N(5)–C(66)	111.7(18)	C(91)–N(8)–C(96)	109.0(17)
C(61)–C(62)	1.56(4)	C(91)–C(92)	1.51(3)	N(5)–C(51)–C(52)	118.5(17)	N(8)–C(81)–C(82)	119.0(20)
C(66)–C(67)	1.53(4)	C(96)–C(97)	1.53(3)	N(5)–C(56)–C(57)	104.1(19)	N(8)–C(86)–C(87)	109.9(19)
				N(5)–C(61)–C(62)	112.8(20)	N(8)–C(91)–C(92)	109.6(18)
				N(5)–C(66)–C(67)	112.3(19)	N(8)–C(96)–C(97)	117.1(18)

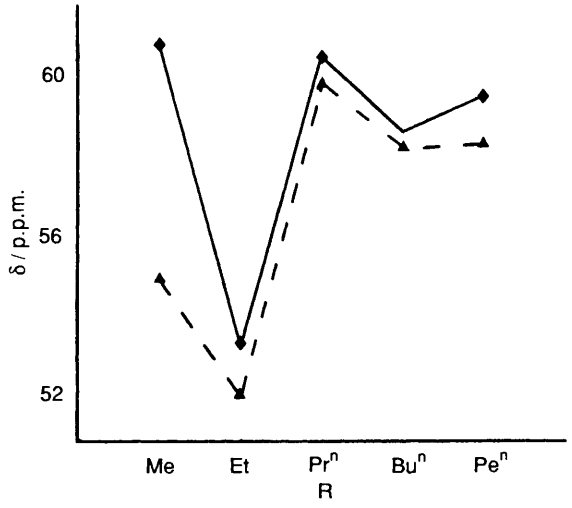

Figure 5. $^{13}C\text{-}\{^1H\}$ Chemical shifts (δ) of the α-carbon atoms for cluster salts $[NR_4]_2[Fe_4S_4(SBu^t)_4]$ (—), and the tetra-alkylammonium halides $[NR_4]Br$ (– – –)

Resolution is poor, too, in the large cavities in the anion–cation framework in the tetrapentylammonium salt. We believe that there are free thiol molecules disordered over several orientations in these regions, but individual molecules have not been identified. In the tetramethylammonium salt too, as has been noted, there are free thiol molecules in the lattice; these molecules are disordered at sites of $\bar{4}2m$ symmetry, with the SH group in any one of the four 'equivalent' positions.

These structures do not give an immediate answer to the question of why there is the observed variation in quadrupole splitting. The close approach of the α-carbon atoms of the alkyl chains to sulphido-sulphur atoms of the cluster invites the suggestion that this might be the route of interaction. However, this would imply that the α-carbon atoms themselves should possess some property which varies in the same way as do the quadrupole splittings.

As a test of this hypothesis, albeit unsatisfactory, we investigated the $^{13}C\text{-}\{^1H\}$ solution n.m.r. chemical shifts of the α-carbon atoms, which are represented in Figure 5. This shows the values obtained both for the cluster salts and the tetra-alkylammonium halides. The shifts vary in the same sense for both sets of salt but not in agreement with the quadrupole splittings, with the steady rise to a maximum at n-propyl. Unfortunately, we could not obtain solid-state spectra, but in any case the ^{13}C shifts do not appear to be the key. The shifts themselves, which seem anomalous, will be discussed in more detail elsewhere.[8]

Another explanation for the quadrupole splittings could be that the iron atoms in the clusters are subjected to the electric field of the positive tetra-alkylammonium ions, and that this field varies with the structure of the salts. The shorter iron–nitrogen separations are shown in Table 8. The differing number of data for the pentylammonium compound is a consequence of the different symmetries and hence independent distances in the crystal. The values for the tetrapropylammonium salt were estimated from the known cell dimensions and the related structures of the tetramethyl- and tetraethyl-ammonium salts. One can rationalize the data on the basis (*a*) that the shorter separations are most significant, and (*b*) that the field of the cation serves to reduce the quadrupole splitting. The electric

Table 7. Final atomic co-ordinates (fractional × 10^4) for $[N(n\text{-}C_5H_{11})_4]_2[Fe_4S_4(SBu^t)_4]\cdot n HSBu^t$ with e.s.d.s in parentheses

Atom	*x*	*y*	*z*	S.o.f*
Fe(1)	7 918(1)	4 257(1)	16(1)	
Fe(2)	7 862(1)	3 473(1)	−842(1)	
Fe(3)	8 819(1)	3 468(1)	−165(1)	
Fe(4)	8 635(1)	4 346(1)	−966(1)	
S(11)	8 819(2)	3 424(3)	−1 139(2)	
S(22)	8 895(2)	4 424(3)	−23(2)	
S(33)	7 657(2)	4 438(3)	−911(2)	
S(44)	7 894(2)	3 306(3)	142(2)	
S(1)	7 395(3)	4 705(3)	706(3)	
C(1)	7 543(11)	5 478(10)	737(12)	
C(11)	6 944(23)	5 763(21)	1 056(22)	0.5
C(12)	7 642(22)	5 714(19)	115(19)	0.5
C(13)	8 079(20)	5 458(18)	1 156(22)	0.5
C(15)	8 182(21)	5 614(20)	718(22)	0.5
C(16)	7 245(21)	5 600(20)	1 367(21)	0.5
C(17)	7 186(22)	5 797(18)	173(18)	0.5
S(2)	7 254(2)	2 988(3)	−1 320(2)	
C(2)	7 256(11)	2 236(10)	−1 063(11)	
C(21)	7 917(21)	2 033(21)	−1 175(22)	0.5
C(22)	6 849(21)	1 958(19)	−1 505(22)	0.5
C(23)	6 993(27)	2 287(26)	−457(26)	0.5
C(25)	7 739(24)	1 904(21)	−850(23)	0.5
C(26)	7 177(25)	1 887(22)	−1 754(26)	0.5
C(27)	6 770(25)	2 100(23)	−652(25)	0.5
S(3)	9 531(3)	2 965(3)	281(3)	
C(3)	9 592(13)	2 220(13)	75(13)	
C(31)	10 369(48)	2 155(44)	239(48)	0.5
C(32)	9 512(36)	2 074(29)	−538(34)	0.5
C(33)	9 111(22)	1 902(20)	361(24)	0.5
C(35)	9 058(36)	1 926(35)	−90(40)	0.5
C(36)	10 004(25)	1 872(23)	408(22)	0.5
C(37)	10 025(33)	2 248(29)	−428(31)	0.5
S(4)	9 089(3)	4 912(3)	−1 621(3)	
C(4)	8 800(13)	5 653(12)	−1 629(12)	
C(41)	8 176(28)	5 809(26)	−1 660(30)	0.5
C(42)	9 101(32)	5 981(30)	−2 223(32)	0.5
C(43)	8 992(36)	6 040(33)	−1 132(35)	0.5
C(45)	8 618(23)	5 820(21)	−976(21)	0.5
C(46)	9 259(24)	6 070(23)	−1 853(27)	0.5
C(47)	8 262(20)	5 603(21)	−2 036(23)	0.5
N(5)	8 258(8)	3 479(9)	7 027(9)	
C(51)	8 510(9)	3 009(9)	7 430(8)	
C(52)	8 821(9)	2 501(10)	7 170(10)	
C(53)	9 129(36)	2 186(34)	7 662(32)	0.5
C(53x)	8 934(24)	2 021(24)	7 608(22)	0.5
C(54)	9 360(17)	1 611(18)	7 418(17)	
C(55)	9 547(24)	1 346(29)	8 054(28)	0.5
C(55x)	9 527(32)	875(37)	7 674(36)	0.5
C(56)	7 887(11)	3 179(10)	6 540(10)	
C(57)	7 400(11)	2 913(11)	6 878(12)	
C(58)	7 022(25)	2 556(26)	6 444(25)	
C(59)	6 702(31)	2 959(34)	6 319(30)	
C(60)	6 344(18)	2 254(19)	5 895(18)	
C(61)	8 707(11)	3 779(10)	6 644(10)	
C(62)	9 180(12)	4 043(12)	6 990(11)	
C(63)	9 426(14)	4 477(14)	6 644(14)	
C(64)	10 063(21)	4 577(22)	6 903(22)	
C(65)	10 161(23)	5 000(25)	6 668(25)	
C(66)	7 918(11)	3 901(11)	7 401(10)	
C(67)	7 612(12)	4 372(11)	7 047(12)	
C(68)	7 189(13)	4 637(12)	7 469(13)	
C(69)	6 688(22)	4 978(20)	7 275(18)	
C(70)	7 008(18)	5 451(17)	7 039(17)	
N(8)	5 804(9)	4 407(9)	−358(9)	
C(81)	6 142(10)	4 856(10)	−668(10)	
C(82)	5 849(11)	5 319(12)	−949(11)	
C(83)	6 274(15)	5 660(17)	−1 226(16)	
C(84)	6 075(29)	6 185(32)	−1 444(30)	0.5
C(84x)	6 392(30)	5 988(33)	−932(31)	0.5
C(85)	6 560(34)	6 490(28)	−1 729(31)	0.5
C(85x)	6 809(31)	6 489(28)	−1 397(34)	0.5
C(86)	5 325(10)	4 659(10)	50(10)	
C(87)	5 592(11)	4 964(10)	534(11)	
C(88)	4 959(36)	5 339(41)	871(36)	0.5
C(88x)	5 060(37)	4 768(41)	1 302(48)	0.5
C(88y)	5 067(31)	5 020(47)	1 054(41)	0.5
C(89)	5 309(37)	5 569(39)	1 276(42)	0.5
C(89y)	5 180(38)	5 262(44)	1 545(39)	0.5
C(90)	4 633(26)	5 291(22)	1 871(24)	0.5
C(91)	5 457(9)	4 082(9)	−807(10)	
C(92)	5 858(11)	3 889(11)	−1 289(11)	
C(93)	5 470(12)	3 355(12)	−1 559(12)	
C(94)	5 824(18)	3 261(19)	−2 166(17)	
C(95)	5 586(20)	2 780(21)	−2 222(19)	
C(96)	6 199(9)	3 980(9)	−48(9)	
C(97)	5 926(11)	3 454(11)	241(12)	
C(98)	6 249(14)	3 193(14)	676(15)	
C(99)	5 944(28)	2 883(34)	1 334(31)	
C(100)	5 979(28)	2 466(33)	1 099(31)	
Atoms of disordered, free thiol molecule				
C(110)	3 383(34)	2 604(31)	4 911(34)	0.3
C(111)	2 610(48)	2 683(51)	4 564(46)	0.3
C(112)	3 577(50)	2 733(44)	4 438(60)	0.3
C(113)	3 265(54)	3 502(56)	5 258(55)	0.3
C(120)	4 425(55)	4 157(62)	4 830(52)	0.3
C(121)	3 519(49)	4 271(55)	5 329(52)	0.3
C(122)	4 741(68)	3 834(58)	4 690(54)	0.3
C(124)	4 721(91)	4 451(74)	5 176(71)	0.3
C(131)	4 866(50)	4 866(50)	4 866(50)	0.3
C(132)	3 873(88)	4 197(92)	2 602(70)	0.3
C(133)	4 061(69)	3 540(51)	4 274(57)	0.3
C(134)	3 788(137)	3 251(109)	2 863(97)	0.3
C(135)	4 666(37)	3 181(36)	3 801(36)	0.3
C(136)	3 097(33)	3 549(58)	3 496(53)	0.3
C(137)	3 085(82)	4 075(83)	3 030(84)	0.3
C(138)	3 368(114)	4 603(99)	2 669(92)	0.3
C(141)	2 870(51)	3 171(47)	4 825(47)	0.3
C(142)	4 367(24)	4 367(24)	4 367(24)	0.3
C(143)	3 571(56)	3 973(55)	5 461(44)	0.3
C(144)	4 097(50)	4 133(46)	5 390(42)	0.3
C(145)	2 725(64)	3 264(81)	3 655(91)	0.3
C(146)	4 327(82)	4 677(88)	5 122(85)	0.3

* Site occupancy factor, if different from 1.0

field gradient V_{zz} depends upon $1/r^3$, where r is the distance of the charge from the iron nucleus. On this basis, a positive charge *ca.* 5 Å from an iron nucleus should have three times the effect of one at 7.5 Å. The cluster cubes occupy special positions in the unit cells, but the individual iron atoms do not. It is therefore easier for rough comparison to refer all distances to the centres of the cubes.

The sums of the inverses of the cubes of the two shortest

Table 8. Iron–cation separations (Å) in the salts $[NR_4]_2[Fe_4S_4(SBu^t)_4]$

R		$Fe_n \cdots N^a$		$Fe_f \cdots N^a$		$Fe^*_4 \cdots N_n{}^b$	$Fe^*_4 \cdots N_{nn}{}^b$
Me		4.966(1)		6.849(1)		5.742[4]	10.756[8]
Et		5.126(1)		7.028(1)		5.915[4]	11.318[8]
Pr^n [c]		5.11		7.00		5.90[4]	12.2[8]
n-C_5H_{11}	N(5)	5.04(2)	5.31(2)	6.76(2)	7.31(2)	5.94	12.42
		5.18(2)	5.37(2)	6.92(2)	7.37(2)	6.05	13.10, *etc.*
	N(8)	5.06(2)	5.32(2)	6.73(2)	7.35(2)	5.95	12.93
		5.26(2)	5.53(2)	6.94(2)	7.56(2)	6.16	13.00, *etc.*

[a] The anions are orientated so that each cation faces the Fe_2S_2 planes of two anions (Figures 3 and 4), giving two N · · · Fe distances to the near face of the anion (Fe^n) and two to the further side (Fe_f). Symmetry in all but the n-pentyl salts reduces the number of independent values. [b] Fe^*_4 is the calculated centre of the four Fe atoms of a cluster, and N_n and N_{nn} represent the nearest and next-nearest nitrogen atoms, respectively. The number of equivalent separations for a given Fe^*_4 centre is shown in square brackets. [c] The values for R = Pr^n are estimated from the dimensions of the Fe_4S_4 core of the methyl salt and the measured cell parameters of the tetrapropylammonium salt. As a check, the values for R = Et were then calculated from those estimated for R = Pr^n, and found to be consistent with those already determined.

Table 9. Mössbauer spectra of some tetrahalogenoferrates $[FeX_4]^{2-}$ (X = Cl or Br) (77 K)

Salt	Isomer shift/ mm s^{-1}	Quadrupole splitting/ mm s^{-1}	Half-width mm s^{-1}
$[NMe_4]_2[FeBr_4]$	0.99(1)	2.07(1)	0.24(2)
$[NEt_4]_2[FeBr_4]$	0.98(1)	2.52(1)	0.34(2)
$[NEt_4]_2[FeBr_4]$*	1.02(>5)	2.29(>5)	0.46
$[NMe_4]_2[FeCl_4]$	1.04(1)	2.62(1)	0.35(1)
$[NMe_4]_2[FeCl_4]$*	1.01(5)	2.61(5)	0.45
$[NEt_4]_2[FeCl_4]$*	1.02(5)	2.68(5)	0.71
$[NBu^n{}_4]_2[FeCl_4]$	1.05(1)	2.70(2)	0.34(2)

* Data from P. R. Edwards, C. E. Johnson, and R. J. P. Williams, *J. Chem. Phys.*, 1967, **47**, 2074

separations (suitably weighted) are 0.028, 0.025, and 0.024, in the order Me > Et > Pr^n, the inverse order of the q.s. values. The $[N(n\text{-}C_5H_{11})_4]^+$ structure is not as easy to evaluate, being much more unsymmetrical. We conclude that the cations are making the major contribution to the significant q_{latt}. These considerations suggest that the half-widths of the spectrum of tetrapentylammonium salt should be larger than the corresponding values for the $[NMe_4]^+$ and $[NEt_4]^+$ salts. This is observed. There should be a solvent effect if we make measurements on frozen solutions. The weighted-average iron–nitrogen separation should be greatest for the tetrapropylammonium salt (see Table 8). We hope eventually to test these predictions. Finally, the effect of charges should not be restricted to cluster compounds, but should be evident in salts of simple mononuclear ions.

Table 9 shows data from some tetrachloroferrates and tetrabromoferrates. They are consistent with literature data for high-spin iron(II) tetrahedral complexes. We do not have enough structural data to attempt an analysis at this stage. However, it does appear that the trend is consistent with what we have observed with the cluster salts, suggesting that the splitting increases as the external positive lattice field decreases. This at least confirms that we have a genuine effect which has not yet been appreciated.

There are few literature data concerning the influence of cations on ^{57}Fe Mössbauer spectral parameters. Woodruff *et al.*[9] reported that the linewidth of the single-line spectra of salts of $[FeCl_4]^-$ increases with cation size. This was rationalized by suggesting that larger cations allow a greater variation in local iron environments, but they did not consider that the wider lines may hold unresolved quadrupole splittings. This is often the case with frozen solutions which can contain several very similar sites with nearly the same q.s.

Clausen and Good[10] followed up this work, but chose to use a range of unsymmetrical cations which also had the potential to hydrogen-bond. They attributed their observations to distortions of the spherical symmetry in their high-spin d^5 anions by the cations, perhaps *via* hydrogen bonding. In our series of $[FeCl_4]^{2-}$ salts, hydrogen bonding is unlikely, yet a cation dependence is still apparent.

Conclusion

We have shown that a field due to positive ions in the lattice of a salt can influence the quadrupole splitting observed in the Mössbauer spectrum. What we can now attempt is to quantify these lattice effects by comparison with the influence of an applied field. We predict that a negative field due to negative ions should have the opposite influence on the quadrupole splitting to that reported here, and we would expect to see a lattice effect in the spectra of other Mössbauer-active atoms, other oxidation states, and other spin states. The effects may not be as large as those seen with clusters as the polarizability and distribution of electrons must exert some influence.

The analysis of the crystal structures of the $Fe_4S_4{}^{2+}$ clusters reveals that the iron–sulphur cores are relatively invariant, though the core–cation distances do differ. Iron–sulphur clusters are involved in many biological electron-transfer processes, and they possess redox potentials which depend in some way on the protein environment. One conceivable way to change redox potentials would be to change the local charges, and this may be the mechanism of control. We are now attempting to test this hypothesis.

Experimental

The clusters $[YR_4]_2[Fe_4S_4(SBu^t)_4]$ (Y = N or P, R = alkyl) and $[NBu^n{}_4]_2[Fe_4Se_4(SBu^t)_4]$ were prepared by standard procedures.[11] The salt $Cs_2[Fe_4S_4(SBu^t)_4]$ was prepared by an adaptation of the standard procedure; a methanolic solution of $[Fe_4S_4(SBu^t)_4]^{2-}$, prepared by mixing iron(III) chloride, sulphur, and 2-methyl-2-propanethiol in methanol, was filtered into a solution of caesium chloride in methanol–water (5:1, v/v). All cluster salts exhibited characteristic ^1H n.m.r. spectra and gave satisfactory elemental analysis. The salts $[YR_4]_2[FeX_4]$ (X = Br or Cl) were isolated from solutions of iron(II) halide and $[YR_4]X$ in ethanol and characterized by elemental analysis.

Proton and $^{13}C\text{-}\{^1H\}$ n.m.r. spectra were recorded on a JEOL GSX270 spectrometer in solution in CD_3CN. Mössbauer spectra were measured at 77 K on a spectrometer previously described[12] and are referenced against natural iron at 278 K.

Crystal Structure Analyses of $[NR_4]_2[Fe_4S_4(SBu^t)_4]$ (R = Me, Pr^n *or* n-C_5H_{11}).—(*i*) $[NMe_4]_2[Fe_4S_4(SBu^t)_4]\cdot HSBu^t$. *Crystal data.* $2C_4H_{12}N\cdot C_{16}H_{36}Fe_4S_8\cdot C_4H_{10}S$, M = 946.8, tetragonal, space group $I\bar{4}2m$ (no. 121), $a = b$ = 11.484(7), c = 18.190(12) Å, U = 2 398.7 Å^3, Z = 2, D_c = 1.308 g cm^{-3}, $F(000)$ = 1 000, μ(Mo-K_α) = 15.8 cm^{-1}, λ(Mo-$K_{\bar{\alpha}}$) = 0.710 69 Å.

Crystals were black square plates. One, *ca.* 0.3 × 0.3 × 0.08 mm, was mounted in air on a glass fibre and coated in silicone grease. After preliminary photographic examination, the crystal was transferred to our Enraf-Nonius CAD4 diffractometer, where accurate cell dimensions were refined from the goniometer settings of 24 strong reflections (θ *ca.* 10.5°).

Diffraction intensities for 363 independent reflections (θ_{max} = 20°) were measured, and corrected for Lorentz–polarization effects, slight deterioration, and absorption, before entry into the SHELX program.[13] The location of the Fe atom was determined from a Patterson synthesis, and the other non-hydrogen atoms were found in subsequent electron-density and difference Fourier maps.

The t-butyl group in the anion is disordered in two orientations with an occupancy ratio of 3:1, and the thiol molecule is disordered equally in the four possible orientations about its position of $\bar{4}2m$ symmetry. The atoms of the thiol molecule and those in the minor orientation of the anionic butyl group were refined isotropically; all other atoms were allowed anisotropic thermal parameters (with symmetry equivalences as appropriate). No hydrogen atoms were included.

Refinement, by full-matrix least-squares methods, converged at R = 0.045, R' = 0.049[13] for all 363 data (*i.e.* omitting no weak, unobserved reflections), weighted $w = (\sigma_F^2 + 0.005\,05\,F^2)^{-1}$. The major peaks (maximum 0.37 e Å^{-3}) in a final difference map were in the region of the disordered anionic butyl group, or in positions likely to correspond to hydrogen atoms.

Scattering factors for neutral atoms were from ref. 14. Computer programs used in this analysis have been noted above or in ref. 15, and were run on the VAX 11/750 machine at AFRC Institute of Horticultural Research (Glasshouse Crops Research Institute) Littlehampton.

(*ii*) $[NPr^n_4]_2[Fe_4S_4(SBu^t)_4]$. *Crystal data.* $2C_{12}H_{28}N\cdot C_{16}H_{36}Fe_4S_8$, M = 1081.0, tetragonal, space group $I\bar{4}2m$ (no. 121), $a = b$ = 11.791(7), c = 21.336(6) Å, U = 2 966.1 Å^3, Z = 2, D_c = 1.210, assuming above formula.

Crystals were very dark coloured. For several crystals examined, diffraction was poor; most were not single crystals and they deteriorated even when coated with silicone grease. Cell parameters, refined from goniometer settings of 24 reflections having θ *ca.* 7.2°, were similar to those of the tetramethyl- and tetraethyl-ammonium salts, with which this sample was assumed to be isostructural.

(*iii*) $[N(n\text{-}C_5H_{11})_4]_2[Fe_4S_4(SBu^t)_4]\cdot n HSBu^t$ (*n ca.* 1). *Crystal data.* $2C_{20}H_{44}N\cdot C_{16}H_{36}Fe_4S_8\cdot nC_4H_{10}S$, M = 1 395.7 assuming n = 1, rhombohedral, space group $R3c$ (no. 161), a = 23.428(5) Å, α = 87.89(2)°, U = 12 833 Å^3, Z = 6, D_c = 1.083 g cm^{-3}, $F(000)$ = 4 536, μ(Mo-K_α) = 9.1 cm^{-1}.

Crystals were well formed, deep red square prisms; several were mounted, in air, on glass fibres and coated with epoxy resin. A photographic and diffractometric procedure similar to that for the tetramethylammonium salt was followed. The crystal was 0.30 × 0.30 × 0.33 mm; cell parameters were refined from the goniometer settings of 25 reflections with θ *ca.* 10.5°; data to $\theta_{max.}$ = 18° were measured (few observable reflections at this level). Corrections were applied for Lorentz-polarization effects, absorption, and negative intensities.

Of the 2 946 unique reflections input to the SHELX program[13] system, 1 996 had $I > 2\sigma_I$. *E*-Statistics shows a mean $E^2 - 1$ value of 0.87, midway between the theoretical values for centro- and non-centro-symmetric lattices. A plausible Fe_4S_8 substituted cubane-type fragment was found by the automated Patterson methods in the SHELXS program,[16] in the non-centrosymmetric space group $R3c$. Electron-density and difference maps based on this fragment yielded the butyl groups and the cations, all of which showed disorder. Many difference peaks remained, assumed to be a much-disordered $HSBu^t$ molecule; some 22 peaks were refined as independent carbon atoms, each with site occupancy 0.3, but the molecules in this region remain mostly unresolved.

Refinement by large-block least-squares methods gave R = 0.062 and R' = 0.058[13] for the 1996 'observed' reflections weighted $w = (\sigma_F^2 + 0.00049\,F^2)^{-1}$. Only the Fe and S atoms were refined with anisotropic thermal parameters.

Additional material available from the Cambridge Crystallographic Data Centre comprises thermal parameters and remaining bond lengths and angles.

Note added at proof. A recent *X*-ray analysis[17] has shown that the tetramethylammonium salt recrystallised from acetonitrite solution has the formula $[NMe_4]_2[Fe_4S_4(SBu^t)_4]\cdot MeCN$.

Crystal data. $2C_4H_{12}N\cdot C_{16}H_{36}Fe_4S_8\cdot C_2H_3N$, M = 897.7, trigonal, space group $P3_121$ (no. 152), $a = b$ = 11.823(1), c = 28.038(2) Å, U = 3 394.3 Å^3, Z = 3, D_c = 1.317 g cm^{-3}, $F(000)$ = 1 416, μ(Mo-K_α) = 16.3 cm^{-1}. Currently R = 0.058, R' = 0.065 for 1 999 reflections with $I > 2\sigma_I$ (of 2 292 independent reflections). The anion has similar conformation, disordered butyl groups, and dimensions to those in Figures 1 and 2, Tables 4 and 6; the $\bar{4}$ axis is not precise, but a two-fold symmetry axis relates (in Figure 2) Fe(1) with Fe(2), S(22) with S(11) *etc.* The packing of cations about the anions shows some similarities with the arrangements in Figures 3 and 4, but the S · · · C_α distances are not as short as those reported above.

References

1 B. A. Averill, T. Herskovitz, R. H. Holm, and J. A. Ibers, *J. Am. Chem. Soc.*, 1973, **95**, 3523.
2 T. G. Spiro (ed.), 'Iron–Sulfur Proteins,' Wiley, New York, 1982.
3 R. N. Mullinger, R. Cammack, K. K. Rao, D. O. Hall, D. P. E. Dickson, C. E. Johnson, J. D. Rush, and A. Simopoulos, *Biochem. J.*, 1975, **151**, 75; C. L. Thompson, C. E. Johnson, D. P. E. Dickson, R. Cammack, D. O. Hall, U Weser, and K. K. Rao, *ibid.*, 1974, **139**, 97; D. P. E. Dickson, C. E. Johnson, R. Cammack, M. C. W. Evans, D. O. Hall, and K. K. Rao, *ibid.*, p. 105.
4 D. J. Evans, G. J. Leigh, A. Houlton, and J. Silver, *Inorg. Chim. Acta*, 1988, **146**, 5.
5 D. J. Evans and G. J. Leigh, *J. Chem. Soc., Chem. Commun.*, 1988, 395.
6 N. N. Greenwood and T. C. Gibb, 'Mössbauer Spectroscopy,' Chapman and Hall, London, 1971.
7 P. K. Masharak, K. S. Hagen, J. T. Spence, and R. H. Holm, *Inorg. Chim. Acta*, 1983, **80**, 157.
8 D. J. Evans, G. J. Leigh, and C. J. Macdonald, unpublished work.
9 R. J. Woodruff, J. L. Mavini, and J. P. Fackler, *Inorg. Chem.*, 1964, **3**, 687.
10 C. A. Clausen and M. L. Good, in 'Mössbauer Effects Methodology,' vol. 4, ed. I. J. Groverman, Plenum, New York, London, 1968, p. 187.
11 G. Christou and C. D. Garner, *J. Chem. Soc., Dalton Trans.*, 1979, 1093.
12 M. Y. Hamed, R. C. Hider, and J. Silver, *Inorg. Chim. Acta*, 1982, **66**, 13.
13 G. M. Sheldrick, SHELX 76, Program for crystal structure determination, University of Cambridge, 1976.
14 'International Tables for *X*-Ray Crystallography,' Kynoch Press, Birmingham, 1974, vol. 4, pp. 99 and 149.
15 S. N. Anderson, R. L. Richards, and D. L. Hughes, *J. Chem. Soc., Dalton Trans.*, 1986, 245.
16 G. M. Sheldrick, in 'Crystallographic Computing 3,' eds. G. M. Sheldrick, C. Krüger, and R. Goddard, Oxford University Press, 1985, pp. 175–189.
17 D. J. Evans, A. Hills, D. L. Hughes, G. J. Leigh, and M. D. Santana, unpublished work.

Received 22*nd January* 1990; *Paper* 0/00337I